**NASA TECHNICAL MEMORANDUM**

NASA TM X-71652

NASA TM X-71652

# THE EFFECTS OF EXPOSURE TO $LN_2$ TEMPERATURES AND 2.5 SUNS SOLAR RADIATION ON 30-CM ION THRUSTER PERFORMANCE

By Michael J. Mirtich
Lewis Research Center
Cleveland, Ohio 44135

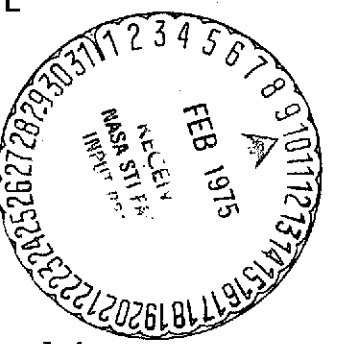


TECHNICAL PAPER to be presented at Eleventh Electric Propulsion Conference sponsored by American Institute of Aeronautics and Astronautics New Orleans, Louisiana, March 19-21, 1975

# THE EFFECTS OF EXPOSURE TO $LN_2$ TEMPERATURES AND 2.5 SUNS SOLAR RADIATION ON 30-CM ION THRUSTER PERFORMANCE

Michael J. Mirtich
Lewis Research Center
National Aeronautics and Space Administration
Cleveland, Ohio

## Abstract

An experimental test program was developed to demonstrate all 30 cm Hg-ion bombardment thruster functions over the thermal environment of several proposed missions. A 30 cm thruster with grids dished 1.25 cm and instrumented with 31 thermocouples, was placed in a vacuum tank equipped with -196° C walls. Cold storage of a thruster was simulated and temperatures as low as -100° C were attained on the thruster. The thruster started successfully from these cold conditions. The thruster operating at both half and full beam power was exposed to 2.5 suns on axis solar simulation. Various thruster thermal configurations, used to simulate multiple thruster operation, were tested at the above conditions. The results of these tests are reported herein.

E-8227

## I. Introduction

An experimental test program was developed to demonstrate all 30 cm Hg-ion bombardment thruster functions over the thermal environments of several proposed missions.(1)(2)(3) Goals of the program were to demonstrate: (1) cold storage and subsequent restart capability with the thruster exposed to temperatures as low as liquid nitrogen (-196° C). (2) that neither transient nor spatial thermal gradients had adverse effects on thruster components or operation. This included the subjecting to thermal shock of certain key thruster components and checking for any problem which may develop. (3) successful thruster operation at both half and full power when exposed to on-axis simulated solar radiation of up to two suns intensity. The purpose of these tests was the documentation of problems which might develop with respect to loss of control of the thruster, high voltage breakdowns induced by variations of the gap of the grids, change in perveance and/or beam profile. (4) the effects of other thrusters operating in close proximity. Another goal of the program was to characterize the thruster as a thermal element in the total spacecraft system.

## II. Apparatus and Procedure

### Facility

To implement this program, it was first necessary to develop a facility capable of providing thruster background temperatures of liquid nitrogen (-196° C). This was accomplished by modifying a 1.5 meter diameter by 6.1 meter long (including the belljar) vacuum tank equipped with four oil-diffusion pumps. This modified tank, along with the position of the thruster in the tank, is sketched in Figure 1. Since this tank had a cylindrical liquid nitrogen ($LN_2$) baffle that was only 4.5 meter long, radiation shielding, consisting of aluminum and aluminized Mylar, was attached to the ends of the $LN_2$ baffle to reduce the thermal loading from the room temperature tank walls (see Fig. 1). The aluminum shielding was spray painted with a layer of graphite to reduce sputtering and provide a better background for solar illumination by reducing reflections. Aluminum and aluminized-Mylar shielding were also placed between the diffusion pumps on the floor of the tank and in places where gaps occurred in the $LN_2$ baffle. This provided reasonably uniform background temperatures for the thruster as indicated by the thermocouple readings shown in Figure 1. Except for the radiation shields at the ends of the baffle, these temperatures remained nearly constant during thruster operation. Temperatures at the upstream radiation shield (behind the thruster) increased due to thermal loading from the operating thruster and the downstream (target) shield increased in temperature from the bombardment of the Hg-ion beam. The target radiation shield had a hole 30 cm in diameter on the tank centerline to allow on-axis solar illumination of the thruster. A double quartz window 26 cm in diameter was located on the centerline of the tank end flange. This window was protected with a movable shield when not in use. The radiation shield behind the thruster (Fig. 2a) had a hole 60 cm in diameter, through which the thruster projected. Figure 2(b) shows the mounted thruster and the mating radiation shield. This shield sealed the hole, in the tank radiation shield, through which was projected the thruster. Figure 3 is a frontal view of the thruster as it was mounted in the vacuum tank.

Thruster mount system and thermocouple locations. A 30 cm diameter 400 series Hughes thruster was extended into the cold environment of the tank. The thruster was supported by four ceramic ($Al_2O_3$) rods 5 cm in diameter by 5 cm long. The ceramic supports served the dual purpose of providing both electrical and partial thermal isolation for the thruster. The ceramic was in turn attached to an aluminum collar to give structural support. This thruster assembly was then attached to the end flange (see Fig. 4) by four, 2.54 cm diameter 183 cm long aluminum rods. The aluminum rods allowed the thruster to extend through the radiation shield and into the tank. Figure 5 is a back view of the thruster looking into the tank. All power leads, propellant feed lines and thermocouple leads came out the back of the thruster and were contained inside the four aluminum rod mount system. This allowed control of any conduction losses incurred by these leads or feed lines. These loses were calculated to be about :70 mw for all thermocouples, 190 mw for the feed lines, 44 mw for the Hg in the feed lines and 2.2 w for the supports.

The thruster shown in Figure 6 had grids with a 1.25 cm dish (43% open area accelerator grid and a 67% open area screen grid) and was instrumented with a total of 31 chromel-alumel (C-A) thermocouples. Twenty thermocouples were at high voltage and located on the Hg feed lines, main and cathode

vaporizes, cathode base, cathode radiation shield, manifold (3), engine body (9), grid assembly, and anode. Eleven thermocouples were located at low voltage: four at various locations on the neutralizer and feed line, five in the ground screen and two on the rear shield. The locations of most of the thermocouples are shown in Figure 7. On the outside of the engine body the thermocouples were located 90° apart, four in the front, four in the center, and one in the rear. Four thermocouples were located 90° apart in the center of the ground screen. The rest of the thermocouple locations are pointed out in Tables I, II and III.

Solar simulation. Shown in Figure 8 is the 40 kw carbon arc lamp used to simulate the sun spectrally at 0.7 A.U. (2 suns intensity). The lamp radiation was collected through a movable quartz lens system and illuminated an area 100 cm in diameter at a distance of 4.2 meters (the distance from the lamp to the thruster). Testing and previous use of the carbon arc lamp is extensively documented in reference 4. In Figure 9 data from reference 4 show that the carbon arc spectrally matches the Johnsen curve for the solar spectrum very closely. These data presented herein were taken with consumable carbon negative and positive electrodes at an intensity setting of 0.140 w/cm$^2$ using a calibrated radiometer at the entrance slit of a spectroradiometer. The solar intensity was measured using the same technique as that employed in reference 5. The short circuit current of a 1 x 2 cm N/P silicon solar cell was used as a radiometer to measure solar intensity. As indicated in reference 5, the short circuit current of a solar cell is linear with intensity to an intensity level of 500 mw/cm$^2$, a value considerably higher than the intensity levels used in these tests. Two different solar cell readings (whose outputs at one sun were known) were used to measure the solar radiation intensity at the grid plane of the thruster. The cells were mounted as shown in Figure 10. One reading was from a set of 3 cells which was fixed and the other reading was from a single N/P silicon cell mounted on a movable rod. In the stored position the solar cells were shielded to reduce any degradation that might result from back sputtered tank wall material.

The solar beam was divergent and more than covered the thruster diameter. At the radiation shield behind the thruster, it measured 100 cm in diameter. The solar illumination at the grid plane of the thruster was non-uniform. Figure 11 shows the variation of solar intensity (number of suns) across the grid plane. The solar intensity drops from 3.1 suns at the neutralizer location to 1.5 suns at the outermost grid holes. On the centerline of the thruster the intensity is 2.5 suns. This non-uniformity in the beam was felt to be desirable for the preliminary tests reported because it presented a more severe test to the grids, namely that of non-uniform thermal loading. The solar intensity with the beam on remained essentially unchanged during thruster operation. Figure 12 shows the variation of solar intensity as measured at the neutralizer location and on the centerline of the grids. Over the 180 minutes recorded here, the intensity level showed little variation with thruster operating time. Also from run to run the same conditions could be duplicated. Thus, no appreciable changes occurred in the performance of the carbon arc lamp, lens system, quartz window, or solar cell detectors.

Thruster thermal environment. Various thruster thermal configurations simulating multiple thruster operation were tested. Three of these configurations are shown in Figure 13. Configuration 1 had no radiation shielding surrounding the thruster and so the thruster surfaces radiated directly to the surrounding cold tank walls. Configuration 2 had a 360° azimuthal heat shield around the thruster to simulate multiple thruster operation, a heat shield in the rear of the thruster, and an additional shield made of aluminized Mylar that was placed between the azimuthal shield and the rear shield to minimize radiation losses from the back and sides of the thruster. Thermal configuration 3 is similar to configuration 2 except that the aluminized Mylar (Al/Mylar) shielding did not come in contact with the 360° azimuthal shield. Three sheets of aluminized Mylar were added to enclose the ground screen in configuration 3 to further reduce heat losses from the thruster. By use of silicon-rubber strip heaters, it was possible to raise the temperature of the azimuthal shield to around 200° C to simulate the temperature of the engine body on an adjacent thruster.(6) To attain a 200° C temperature on the azimuthal shield required an input power of about 45 watts. The rear shield was also made of aluminum and had C-A thermocouples strategically located to indicate shield temperatures. The aluminized-Mylar heat shielding was made of 0.0012 cm thick Mylar, coated on both sides with 1000 Å of aluminum. The aluminized-Mylar radiation shields in configuration 2 and 3, other than the ground screen shields, consisted of six concentric cylinders.

## III. Results and Discussion

### Component Tests

Prior to testing the total thruster system, several cathode-vaporizer assemblies were cooled to temperatures below -39° C so that the mercury (Hg) in the feed lines was frozen. These tests by Rawlin indicated no physical damage occurred to the cathode-vaporizer assembly even after several cold-soaks.(7)

A main isolator and an isolator from a cathode-isolator-vaporizer assembly were subjected to thermal shock tests. Both isolators were immersed in $LN_2$ until they reached -196° C. The isolators were then removed from the $LN_2$ and immersed in boiling water. No structural damage to the $Al_2O_3$-metal braze was observed. Both isolators were then pressurized to 90 psi and found to have no leaks. These tests demonstrated that isolators could survive transient thermal extremes more severe than those that might be encountered in the proposed mission set.(1)(2)(3)

### Cold-Soak

The 30-cm diameter 400 series thruster in thermal test configuration I was cold soak tested by exposing it to the $LN_2$ cooled walls of the tank. Some of the cold storage temperatures attained on the thruster are shown in Figure 14. The thruster was also cold soaked in thermal test configurations 2 and 3. In all cases, the Hg in the feed lines was frozen at all three vaporizers and 30 cm upstream of the vaporizers. The coldest thruster temperatures attained was -100° C at the neutrali-

zer vaporizer for test configuration 1. Reaching cold soak equilibrium temperatures usually took 14 hours although the thruster could be cooled to within 10° of the final equilibrium temperature in 5 hours. The thruster was cold soaked a total of 20 times. There were no structural changes in the thruster as the result of cold soak tests.

Thruster Startup From Cold Soak

The thruster was started from cold soak temperatures a total of 16 times. Figure 15 shows a typical temperature profile for thermal test configuration 1 on startup at the thermocouple locations depicted in Figure 14. Initially, 60 watts was applied to the tip heaters of the cathode and neutralizers and 45 watts to the main isolators. The thermal feed back from the tip heaters to the neutralizer and cathode vaporizers caused a rapid rise in temperatures at the vaporizers, such that after five minutes the temperature at the neutralizer vaporizer was +40° C and the cathode vaporizer +19° C. After five minutes, the Hg at the main vaporizer was also unfrozen (-37° C). It was not as warm as at the neutralizer and cathode vaporizers because of the large thermal mass of the isolator. For the first 20 minutes the main vaporizer temperatures lagged the other vaporizers temperatures by five minutes. The neutralizer lit after fifteen minutes even without any power applied to the vaporizer or with the Hg still frozen (-62° C) in the feed line 30 cm from the vaporizer. Fifteen minutes after the initial application of power, the neutralizer vaporizer power was set at 1 watt. The cathode vaporizer power was set at 2 watts at 25 minutes and two minutes later the cathode lit. Mercury was still frozen in the feed lines 30 minutes after the initial application of power. After 35 minutes Hg in both the main and cathode feed lines thawed, whereas the Hg in the neutralizer feed line was still frozen (-50° C). After 40 minutes the discharge coupled. The power dissipated in the discharge caused a rapid rise in temperature of the engine body, which in turn helped to thaw the neutralizer feed line after 55 minutes.

It was not always necessary to have a discharge to thaw the neutralizer feed line. At other times it was possible to thaw the Hg in both the main and the neutralizer feed line 30 cm from the vaporizers with only the heat from the main cathode keeper discharge. However, because of its relative thermal isolation from the rest of the thruster, lighting the neutralizer only is not sufficient to thaw the Hg in the cathode and main feed lines. In fact, if the neutralizer by itself is started, the thermal feed back to the neutralizer feed line is insufficient to thaw the Hg and eventually, due to lack of Hg, the neutralizer goes out. This suggests that the neutralizer feed line may need an auxiliary heater or other source of heat to prevent the freezing of Hg in the line.

Solar-Multiple Thruster Simulation Tests

Presented in Table I are the results of the multiple thruster-solar simulation tests. Seven different tests were run with the three thermal configurations shown in Figure 13. The first five tests were run at an ion beam current ($J_B$) = 1.9 amps and tests six and seven at ($J_B$) = 1.0 amps. For ease of comparison, not all of the thruster temperatures are given in Table I. An expanded version, including all the thermocouples on the thruster, is presented in Table II.

The object of the tests was to operate a 30 cm thruster at both full and half beam power and determine the effects of the local environment on closed loop control and operation of the thruster. To accomplish this objective, it was necessary to hold certain thruster parameters constant, namely, beam current ($J_B$) = 1.9 amps, emission current ($J_\varepsilon$) = 10.1 amps, discharge voltage ($\Delta V_I$) ≅ 37 volts, and the neutralizer common voltage to ground $V_g$ = 10.4 volts or $J_B$ = 1 amp, $J_\varepsilon$ = 6.1 amp $\Delta V_I$ = 37.2 volts for half beam power. To keep the above thruster parameters constant, it was necessary to maintain the Hg flows, and hence the vaporizer temperatures, constant. For full beam power, the vaporizer temperatures were $T_{MV}$ = 302° C, $T_{KV}$ = 296° C and $T_{NV}$ = 290° C. Depending on the local thermal environment, the power settings were adjusted to the main, cathode and neutralizer vaporizers. These data are presented in Table I, and show the power settings of the vaporizers for each of the environmental test conditions.

The method used to obtain thruster temperature data was to allow the thruster to attain thermal equilibrium at full beam power with no solar illumination. The solar simulator was then turned on and the associated changes in temperatures at various thruster locations recorded. After 2.5 hours of solar illumination of the thruster and associated changes in power settings of the vaporizers, the thruster appeared to attain thermal equilibrium. These temperature values are presented in Tables I and II.

Test 1 can be considered the baseline case, with no radiation shielding on the thruster and no illumination by on-axis radiation. Tests 2 and 3 had the same thruster thermal configuration (2), but different total environmental conditions. For test 3, 2.5 suns on-axis solar radiation was incident on the centerline of the thruster grid plane. Associated rises in temperatures of the azimuthal, rear, and Al/Mylar shields in between are shown in Table I along with the rise in temperatures of certain other locations on the thruster. Associated with these temperature increases is a reduction in power to the main, cathode and neutralizer vaporizers. Even for the extreme thermal conditions of this test configuration (where the sun was allowed to propagate between the annulus formed by the thruster and the azimuthal shield, relfect off the Al/Mylar and rear shield, and illuminate the back of the thruster) the reduction in power at the vaporizers was small and presented no problem to maintain control of the thruster.

Tests 4 and 5 were run with thermal configuration 3. Test 4 used no solar simulation and test 5 had 2.5 suns incident in the thruster. Wrapping the ground screen with aluminized Mylar and not allowing the ground screen or the rear of the thruster any significant view factor to cold tank walls, further increased temperatures of the metal surfaces on the thruster. To maintain constant thruster conditions, there were further small reductions in power settings at the vaporizers. However, the new power settings even with 2.5 suns solar radiation (as in test 5) still allowed complete control of the thruster. This

test thus indicates that a 400 series thruster could be thermally isolated from the spacecraft if desired.

Also shown in Table I are the data for $J_B$ = 1.0 amps for thermal configuration 3. In tests 6 and 7, to maintain $J_B$ = 1.0 amps, $J_\epsilon$ = 6.1 amps and $\Delta V_I$ = 37.2 volts the temperatures at the cathode and main vaporizers were held at 280° C and 284° C, respectively. At half beam power the cathode and neutralizer discharge powers were lower than at full beam power and consequently there was less thermal feedback to the vaporizers. This can be seen by comparing test 6 ($J_B$ = 1.0 amp) with test 4 ($J_B$ = 1.9 amp) for no solar illumination. The vaporizer power settings were higher in test 6 than in test 4 even though the vaporizer temperatures were lower. The power setting for the main vaporizer was the same at both beam power levels although the vaporizer temperature was lower at half beam power. As Table I shows, the same trends were true for the cathode and neutralizer vaporizers in tests 5 and 7 with 2.5 suns solar illumination and approximately the same for the main vaporizer. Although illuminating the thruster with solar radiation for $J_B$ = 1 amp caused increased thruster body temperatures and a reduction in power settings at the vaporizers, no loss of control of the thruster occurred. In fact with solar illumination, there was a greater margin for reduction in power setting at the vaporizer for the $J_B$ = 1 amp case than for the $J_B$ = 1.9 amp. These trends occurred because the total power into the thruster (discharge power, plus solar illumination) was less for 1 amp than for $J_B$ = 1.9 amps.

Table II lists the temperatures of all 31 thermocouples that were located in the thruster for various test conditions. The thermocouple on the neutralizer tip became unattached during test 1, and was subsequently moved back to a position in front of the collar. The thermocouple designated "anode front" only worked for test 4. For this test, it showed that the temperature of the anode at the front of the thruster was about 78° C hotter than at the rear of the anode. The thruster body thermocouples located at 180° front, center and back also indicated warmer temperatures in the front of the thruster, although the temperature in the center and back of the engine body were the same.

Thruster Grid Performance

In Figure 11 it was shown that the solar intensity across the grid plane was uneven. This non-uniformity is a rather severe test for the grids. Uneven thermal loading of the grids could cause thermal warping[8] and consequent high voltage breakdowns, change in perveance or beam profile. No high voltage breakdowns were observed during solar simulation.

Shown in Figure 16 is a plot of the ratio of the drain current to the beam current ($J_A/J_B$) verses total accelerating voltage for a beam current of 1.9 amps, with and without solar illumination of the grids. This data indicates no change in perveance due to solar heating of the accelerator grid, i.e., no change in grid spacing.

Changes in grid gap can also cause changes in beam profile. A profile measurement was made with a 1.25 cm diameter moly button probe located 1.0 m downstream of the thruster. The probe could only be moved to cover a little over half the beam. This data is shown in Figure 17, for $J_B$ = 1.9 amps with no solar illumination and with 2.5 suns on the centerline of grids. No change in beam profile was detected.

Thus, as on-axis non-uniform solar illumination caused no high voltage breakdowns, no change in grid perveance, and no change in beam profile, there was no evidence of thermal warping of the grids.

Eclipse Simulation

In some proposed missions the spacecraft-thruster system will experience eclipses for durations up to a maximum of 72 minutes. Although exact simulation of an eclipse in the laboratory is difficult, an attempt was made to simulate eclipse conditions using the available thruster, vacuum tank, and sun simulator. The procedure followed was to let the thruster approach thermal equilibrium at full beam power with one sun solar radiation. To simulate an eclipse, the sun simulator and all power to the thruster were turned off at the same time and the temperatures on the thruster recorded. Presented in Figure 18 are cooling curves for the three vaporizers during a simulated eclipse for both the shielded test configuration 3 and the unshielded test configuration 1. In the shielded thruster configuration 3, the main and cathode vaporizers cool at the same rate and after 72 minutes are about 137° C. The neutralizer, isolated from the thermal mass of the thruster, cooled fastest and reached 57° C in 72 minutes. In the unshielded thermal configuration 1, all three vaporizers cooled at different rates, with the neutralizer vaporizer cooling quickest and reaching the lowest temperature (-14° C). In either thermal configuration, there was insufficient time to freeze Hg at the vaporizers.

To simulate a thruster coming out of an eclipse and to test restartability, the solar simulator was turned on after 72 minutes and 60 watts of power applied to the cathode tip heaters in the thruster with thermal configuration 3. Eleven minutes later, the cathodes lit and a discharge attained. Sixteen minutes after coming out of the eclipse the thruster was operating at full beam power conditions ($J_B$ = 1.9 amps, $J_\epsilon$ = 10 amps, $\Delta V_I$ = 37 volts).

Tests by Bechtel[9] on an engineering model thruster show that a determining factor in restarting a thruster, in addition to the vaporizer temperatures, is the temperature of the isolators. Isolator temperatures were not monitored in the series of tests with the 400 series thruster but do follow vaporizer temperatures quite closely.

It would appear from these studies that little or no thermal problems arise during an eclipse for either thermal configuration. However, in the unshielded configuration, the neutralizer vaporizer cooled rapidly during the eclipse simulation and was approaching the freezing point of Hg. This was a simulated eclipse and does not totally represent the background sink temperatures that the spacecraft-thruster system will experience in space. It may be desirable to provide radiation

shielding to the neutralizer and its feed line or install a heater in the Hg feed line if the thruster is flown thermally unshielded. In earth orbit the shielding in thermal configuration 3 prevents any possibility of freezing Hg and may be a desirable flight design feature.

## IV. Concluding Remarks

Cold storage of a 400 series, 30 cm diameter thruster was simulated by mounting a thruster in a vacuum tank with $LN_2$ walls. Thruster metal temperatures were reduced to -100° C. Hg was frozen in the feed lines to a length at least 30 cm upstream of the vaporizers. No structural changes resulted during or after cold storage and the thruster was restarted without any noticeable problems.

No structural changes were found when isolators were subjected to thermal shock. Transient and spatial thermal gradients had no adverse effects on thruster components or thruster operation.

The thruster operated satisfactorily at both half and full beam power when exposed to greater than 2 suns on-axis solar radiation. No problems with respect to loss of control of the thruster, high voltage breakdowns, change in perveance, or beam profile were observed. A simulated multiple thruster configuration showed that thrusters operating in close proximity do not present thermal problems.

It may be desirable for eclipse operation, to thermally shield the thruster from the cold temperatures of space to prevent any possibility of freezing Hg in the feed lines.

In Conclusion:

The thruster was thermally characterized.

It was shown that a thruster may be thermally isolated from the spacecraft, if desired.

All thruster functions were demonstrated over the thermal extremes postulated.

It was also shown that thruster performance was insensitive to the local thermal environment. Enough margin existed in the power setting at the vaporizers to maintain closed loop control.

The data obtained on this thruster could be used to thermally design a thruster to operate satisfactorily at 2 suns solar radiation and -196° C background temperatures.

From the tests performed on this thruster there were no indications of impact on thruster lifetime.

## References


1. Wen, L. C. and Womack, J. R., "Thruster Array Thermal Control," AIAA Paper 73-1117, Lake Tahoe, Nev. 1973.

2. Horio, S. P. and Gutter, C. H., "SEP Stage for Earth Orbital Missions Solar Electric Propulsion Stage for Shuttle/Tug Payload Increase," AIAA Paper 73-1123, Lake Tahoe, Nev., 1973.

3. Ruttner, L. E., "Thermal Control of the Solar Electric Propulsion Stage," AIAA Paper 73-1118, Lake Tahoe, Nev., 1973.

4. Jack, J. R. and Spisz, E. W., "Environmental Simulation from 0.01 to 100 Solar Constants," presented at 6th Space Simulation Conf., New York, May 1-4, 1972.

5. Spisz, E. E. and Robson, R. R., "Silicon Solar Cell as a High-Solar-Intensity Radiometer," TM X-2412, 1971, NASA.

6. King, H. L., Peoschel, R. L., and Schalker, D. E., "An Engineering Model 30 Cm Ion Thruster," AIAA Paper 73-1084, Lake Tahoe, Nev., 1973.

7. Rawlin, Vince, Private communication; data to be published.

8. Rawlin, V., Banks, B. A., and Byers, D. C., "Design, Fabrication, and Operation of Dished Accelerator Grids on a 30-Cm Ion Thruster," AIAA Paper 72-486, Bethesda, Md., 1972.

9. Bechtel, R. L., "Control Logic for a 30-cm Diameter Ion Thruster," AIAA Paper 75-378, New Orleans, La., 1975.

Table I. Solar-multiple thruster simulation tests

| Environment | | | | | | |
|---|---|---|---|---|---|---|
| Test | Thermal configuration | Sun simulation, number of suns | Azimuthal shield | | Rear shield, °C | Al/Mylar shield, °C |
| | | | Type, deg | Temperature, °C | | |
| 1 | 1 | --- | None | None | --- | --- |
| 2 | 2 | --- | 360 | 215 | 140 | 155 |
| 3 | 2 | 2.5 | 360 | 247 | 157 | 191 |
| 4 | 3 | --- | 360 | 218 | 120 | --- |
| 5 | 3 | 2.5 | 360 | 230 | 129 | --- |
| 6 | 3 | --- | 360 | 212 | 98 | --- |
| 7 | 3 | 2.5 | 360 | 220 | 105 | --- |

| Test | | Thruster conditions | | | Conditions at vaporizers | | | | | | Temperatures, °C, on thruster | | | | | | |
|---|---|---|---|---|---|---|---|---|---|---|---|---|---|---|---|---|---|
| | Configuration | $J_B$, A | $J_E$, A | $\Delta V_I$, V | Neutralizer $T_{NV}$ = 290° C | | Cathode $T_{KV}$ = 296° C | | Main $T_{MV}$ = 302° C | | Ground screen (center) | Ground shield (mask) | Engine body center | Engine body front | Anode | Rear shield outer | Cathode base |
| | | | | | $J_{NV}$, A | $V_{NV}$, V | $J_{KV}$, A | $V_{KV}$, V | $J_{MV}$, A | $V_{MV}$, V | | | | | | | |
| 1 | 1 | 1.9 | 10.1 | 36.8 | 1.16 | 3.44 | 1.16 | 3.4 | 1.08 | 6.8 | 84 | 62 | 205 | 262 | 270 | 124 | 379 |
| 2 | 2 | 1.9 | 10.1 | 37.6 | 1.12 | 3.33 | 1.12 | 3.16 | 1.04 | 6.4 | 186 | 111 | 240 | 275 | 285 | 204 | 377 |
| 3 | 2 | 1.9 | 10.1 | 37.6 | .96 | 2.85 | 1.0 | 2.84 | .92 | 6.0 | 219 | 185 | 264 | 305 | 311 | 234 | 386 |
| 4 | 3 | 1.9 | 10.1 | 37.2 | 1.16 | 3.44 | .84 | 2.36 | 1.00 | 6.2 | 258 | 135 | 280 | 300 | 304 | 222 | 379 |
| 5 | 3 | 1.9 | 10.1 | 37.2 | 1.12 | 3.33 | .68 | 1.84 | .96 | 6.1 | 274 | 198 | 297 | 318 | 323 | 242 | 396 |
| | | | | | $T_{NV}$ = 280° C | | $T_{KV}$ = 280° C | | $T_{MV}$ = 284° C | | | | | | | | |
| 6 | 3 | 1.0 | 6.1 | 37.2 | 1.40 | 4.2 | 1.00 | 2.84 | 1.00 | 6.2 | 199 | 96 | 220 | 235 | 242 | 178 | 346 |
| 7 | 3 | 1.0 | 6.1 | 37.2 | 1.24 | 3.68 | .88 | 2.50 | .92 | 6.0 | 225 | 166 | 245 | 260 | 265 | 201 | 363 |

Table II. Thruster temperature levels for test conditions defined in table I, $^{o}C$

| Thermocouple location | Test number | | | | | | |
|---|---|---|---|---|---|---|---|
| | 1 | 2 | 3 | 4 | 5 | 6 | 7 |
| | Thermal configuration | | | | | | |
| | 1 | 2 | 2 | 3 | 3 | 3 | 3 |
| Main vaporizer | 302 | 303 | 302 | 302 | 303 | 284 | 284 |
| Manifold near vaporizer | 247 | 262 | 297 | 281 | 305 | 229 | 256 |
| Manifold 90° from vaporizer | 254 | 268 | 298 | 284 | 307 | 232 | 259 |
| Manifold 180° from vaporizer | 255 | 270 | 296 | 285 | 307 | 234 | 259 |
| Cathode vaporizer | 296 | 296 | 296 | 296 | 297 | 280 | 280 |
| Cathode base | 379 | 377 | 386 | 379 | 396 | 346 | 363 |
| Cathode radiation shield | 184 | 221 | 243 | 223 | 237 | 188 | 203 |
| Cathode 12 in. upstream | 61 | 167 | 199 | 168 | 178 | 138 | 149 |
| Grid assembly | 198 | 230 | 257 | | | | |
| Engine body | | | | | | | |
| Top center | 204 | 240 | 273 | 273 | 293 | 218 | 243 |
| Top front | 253 | 272 | 304 | 295 | 316 | 232 | 258 |
| 90° center | 202 | 241 | 268 | 277 | 296 | 219 | 245 |
| 90° front | 250 | 265 | 288 | 293 | 312 | 230 | 256 |
| 180° back | 205 | 241 | 266 | 277 | 294 | 220 | 243 |
| 180° center | 205 | 240 | 264 | 280 | 297 | 223 | 246 |
| 180° front | 262 | 278 | 305 | 309 | 324 | 242 | 264 |
| 270° center | 207 | 243 | 274 | 280 | 299 | 223 | 247 |
| 270° front | 264 | 283 | 313 | 305 | 323 | 239 | 262 |
| Ground shield (mask) 90° | 62 | 111 | 185 | 135 | 198 | 96 | 166 |
| Ground screen | | | | | | | |
| Top center | 96 | 194 | 242 | 240 | 263 | 192 | 219 |
| 90° center | 85 | 185 | 228 | 253 | 274 | 199 | 227 |
| 180° center | 84 | 182 | 219 | 258 | 276 | 205 | 228 |
| 270° center | 82 | 185 | 219 | 253 | 274 | 200 | 226 |
| Rear shield - out | 124 | 204 | 234 | 222 | 242 | 178 | 201 |
| Rear shield - in | 158 | 219 | 234 | 223 | 239 | 183 | 199 |
| Anode - front | | | | 382 | | | |
| Anode - back | 270 | 285 | 311 | 304 | 323 | 242 | 265 |
| Neutralizer tip | 726 | 458 | 468 | 427 | 440 | 400 | 407 |
| Neutralizer collar | 301 | 364 | 382 | 364 | 372 | 352 | 356 |
| Neutralizer vaporizer | 290 | 291 | 291 | 289 | 289 | 280 | 281 |
| Neutralizer Hg feed line, 16 in. upstream | 68 | 183 | 205 | 174 | 185 | 143 | 155 |

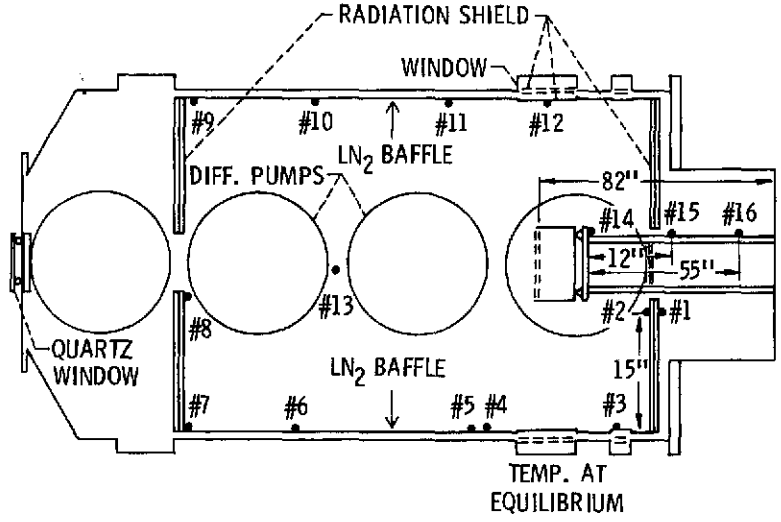


Figure 1. - Vacuum tank, thruster position and tank wall temperatures.

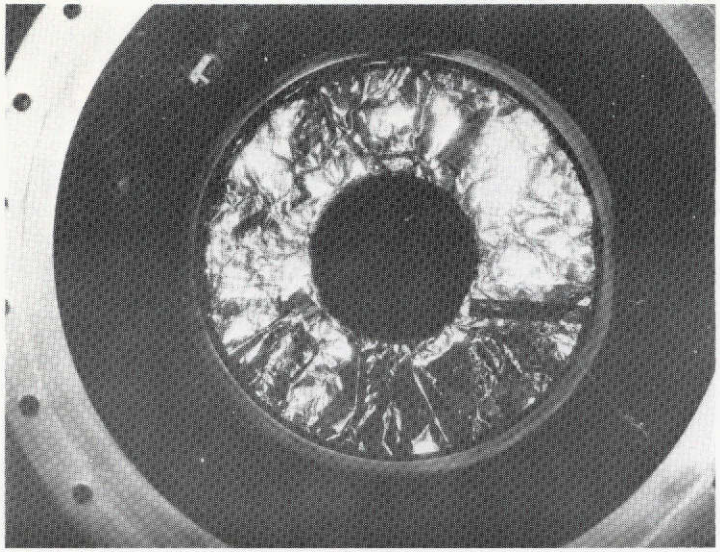

(a)

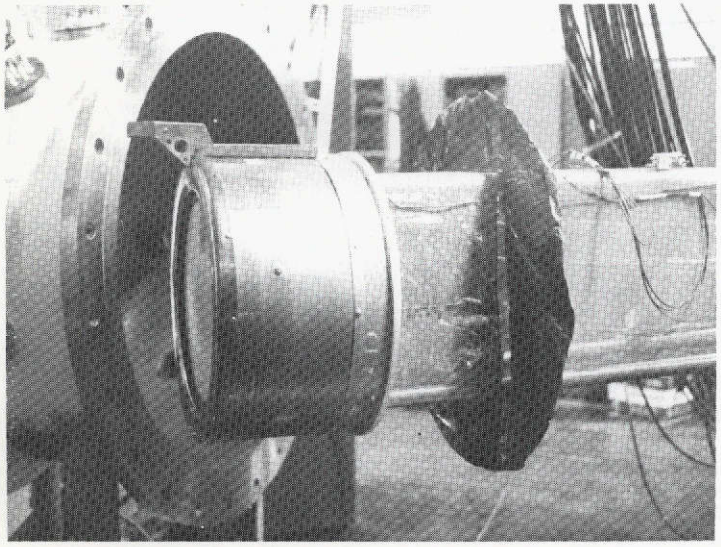

(b)

Figure 2. - View of radiation shield and mounted thruster with mating radiation shield.

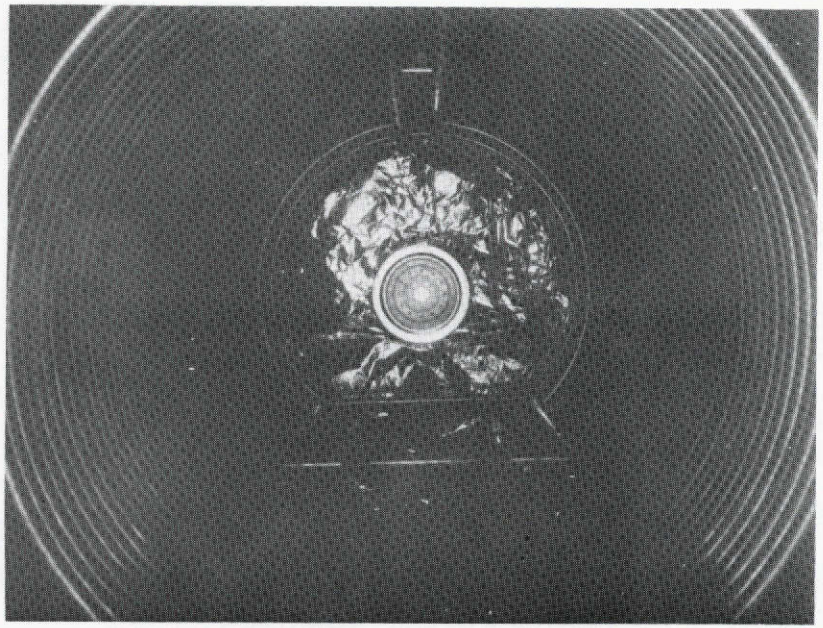

Figure 3. - Frontal view of thruster mounted in vacuum tank.

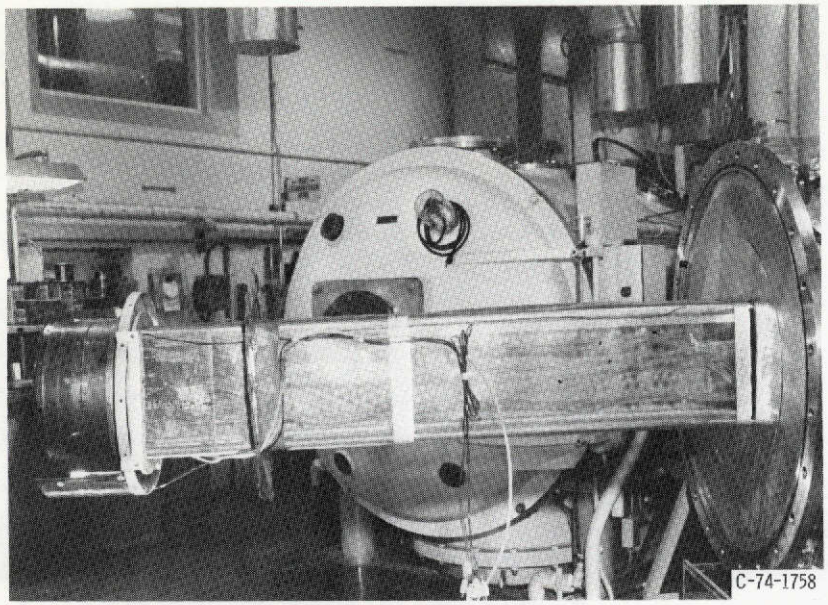


Figure 4. - Thruster, its mount system and flange to which it is attached.

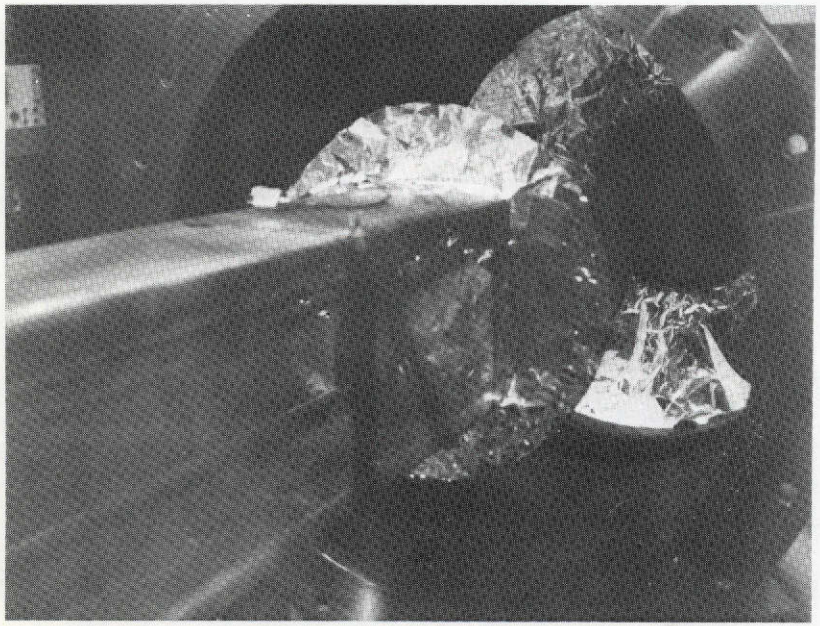

Figure 5. - Back view of thruster looking into tank.

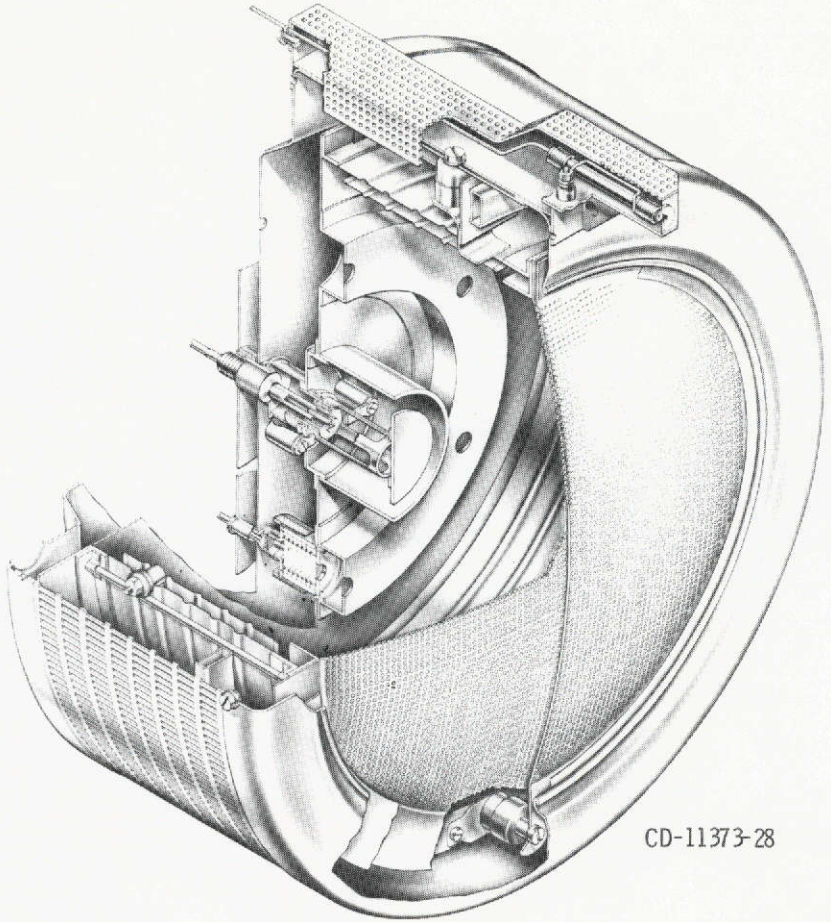


Figure 6. - Hughes 400 series 30 cm thruster with 1.25 cm dished grids.

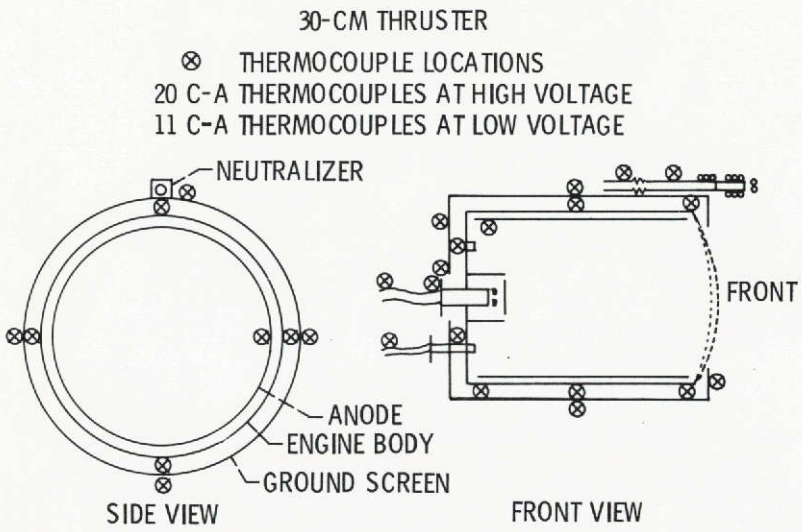


Figure 7. - Sketch of thermocouple locations on thruster.

E-8227

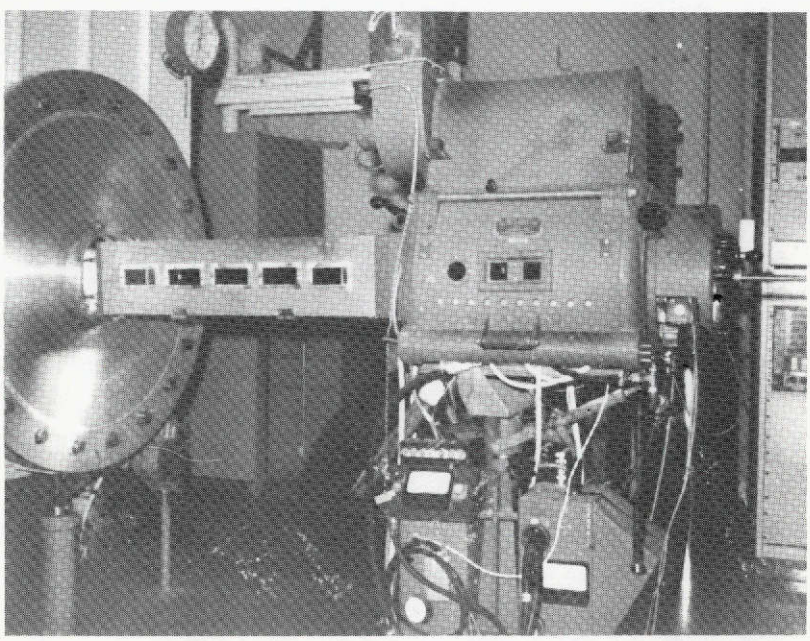

Figure 8. 40 kW Carbon arc solar simulator.

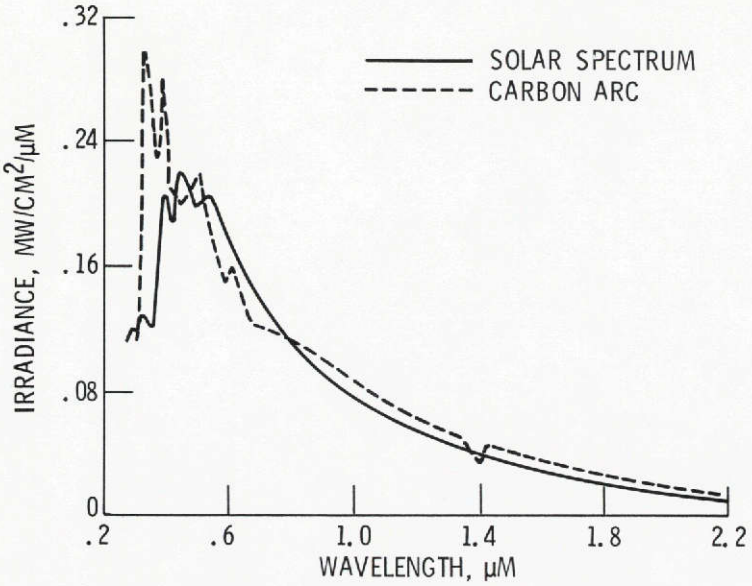


Figure 9. - Spectral irradiance of carbon arc.

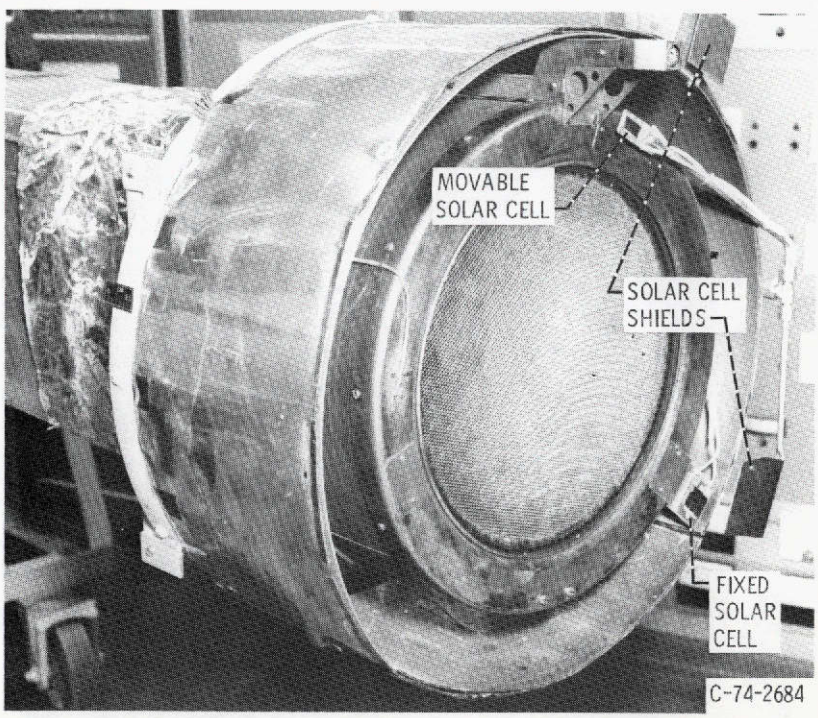


Figure 10. - Solar cells mounted on thruster. Thermal configuration 3.

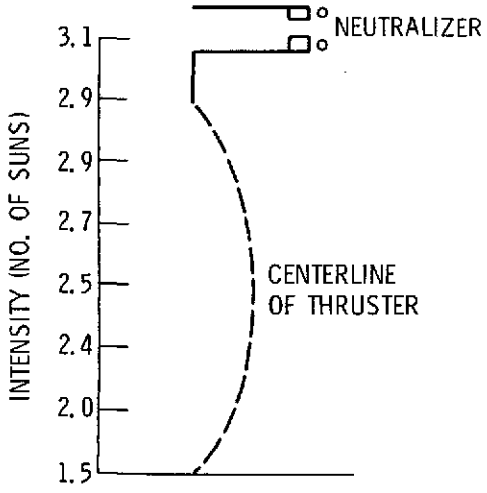


Figure 11. - Variation of illumination at the thruster grid plane.

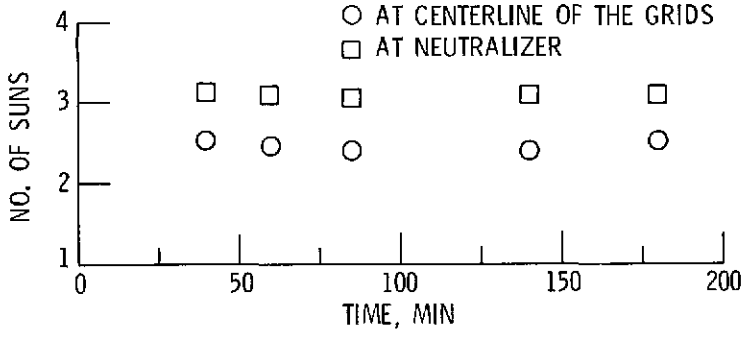


Figure 12. - Variation of solar intensity vs time.

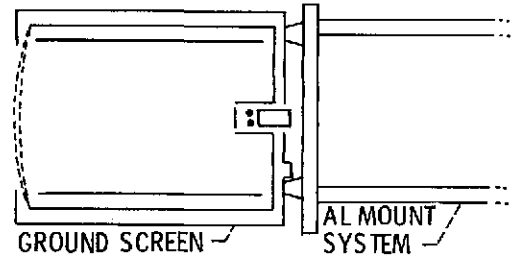


THRUSTER THERMAL CONFIGURATION #1
(NO SHIELDING AROUND THRUSTER)

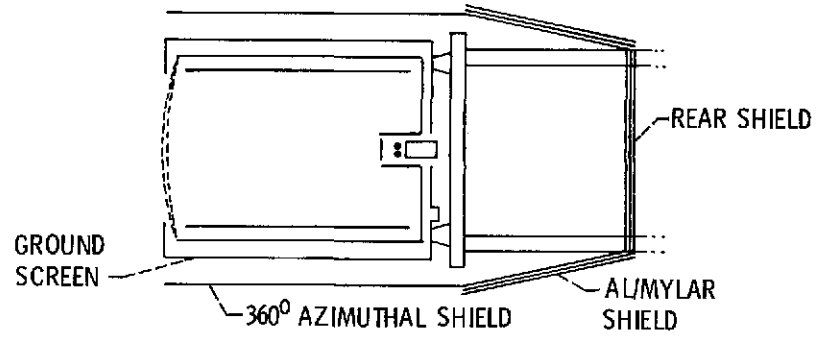


THERMAL CONFIGURATION #2
360° AZIMUTHAL SHIELD + REAR SHIELD + AL/MYLAR SHIELD

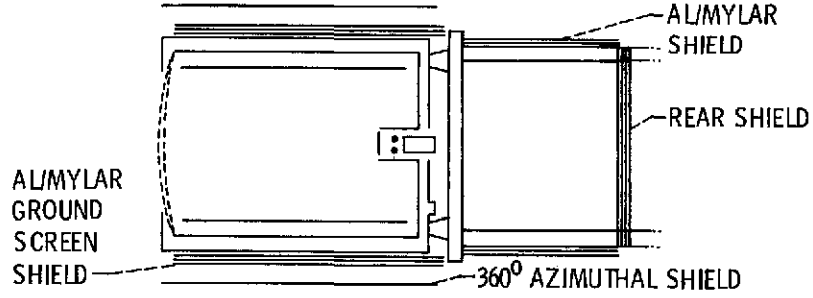


THRUSTER THERMAL CONFIGURATION #3

360° AZIMUTHAL SHIELD + REAR SHIELD + AL/MYLAR SHIELD + AL/MYLAR SHIELD AROUND GROUND SCREEN

Figure 13. - Thruster thermal configurations used in the thermal tests.

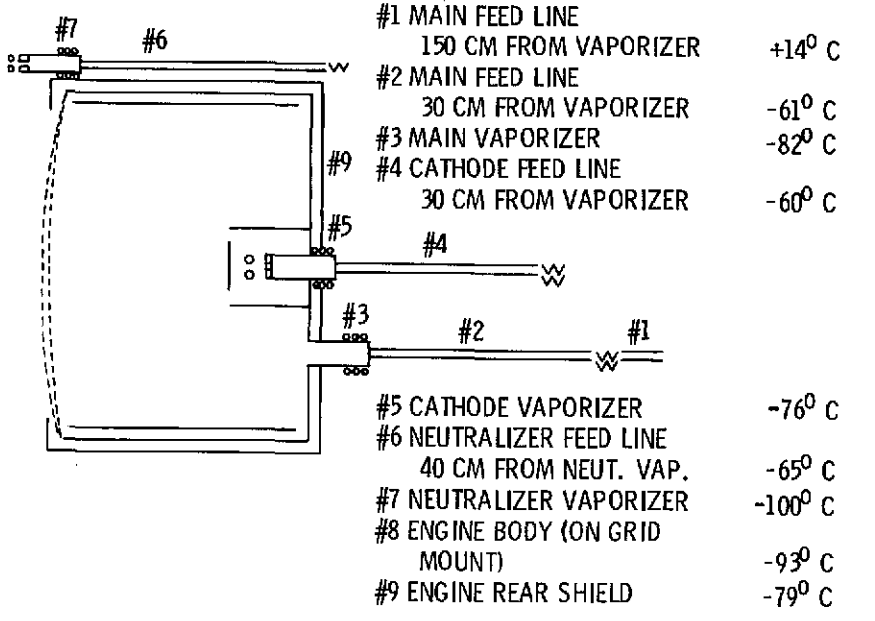


| THERMOCOUPLE LOCATIONS | LOWEST TEMPERATURE |
|---|---|
| #1 MAIN FEED LINE 150 CM FROM VAPORIZER | +14° C |
| #2 MAIN FEED LINE 30 CM FROM VAPORIZER | -61° C |
| #3 MAIN VAPORIZER | -82° C |
| #4 CATHODE FEED LINE 30 CM FROM VAPORIZER | -60° C |
| #5 CATHODE VAPORIZER | -76° C |
| #6 NEUTRALIZER FEED LINE 40 CM FROM NEUT. VAP. | -65° C |
| #7 NEUTRALIZER VAPORIZER | -100° C |
| #8 ENGINE BODY (ON GRID MOUNT) | -93° C |
| #9 ENGINE REAR SHIELD | -79° C |

Figure 14. - Cold storage temperatures for thermal configuration 1.

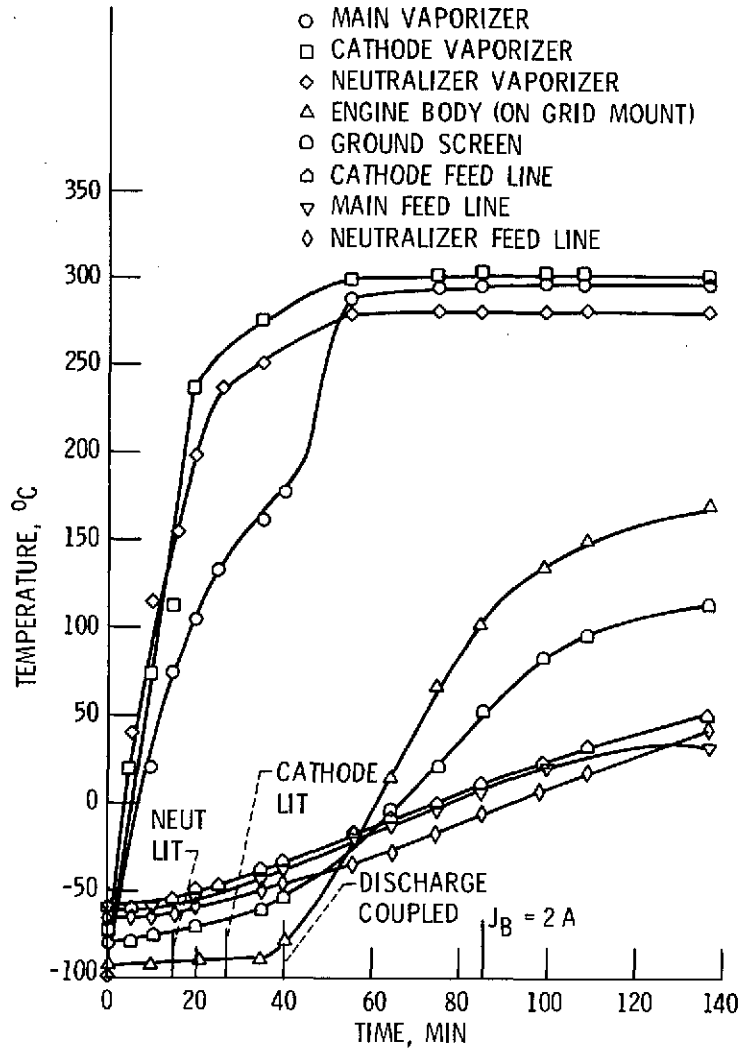


Figure 15. - Temperature profiles on startup for a thruster in thermal configuration 1 from cold storage.

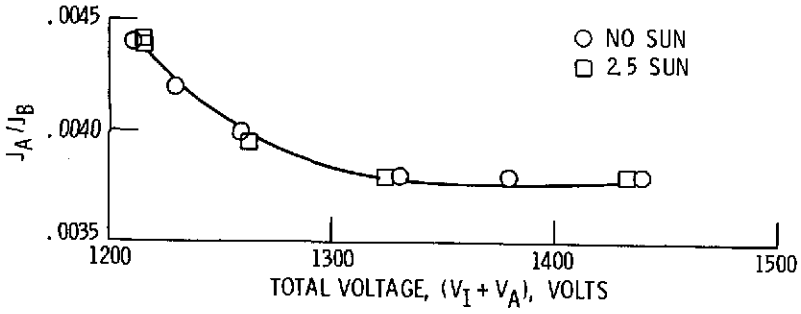


Figure 16. - Plot of $J_A/J_B$ vs total voltage, for $J_B$ = 1.9 A.

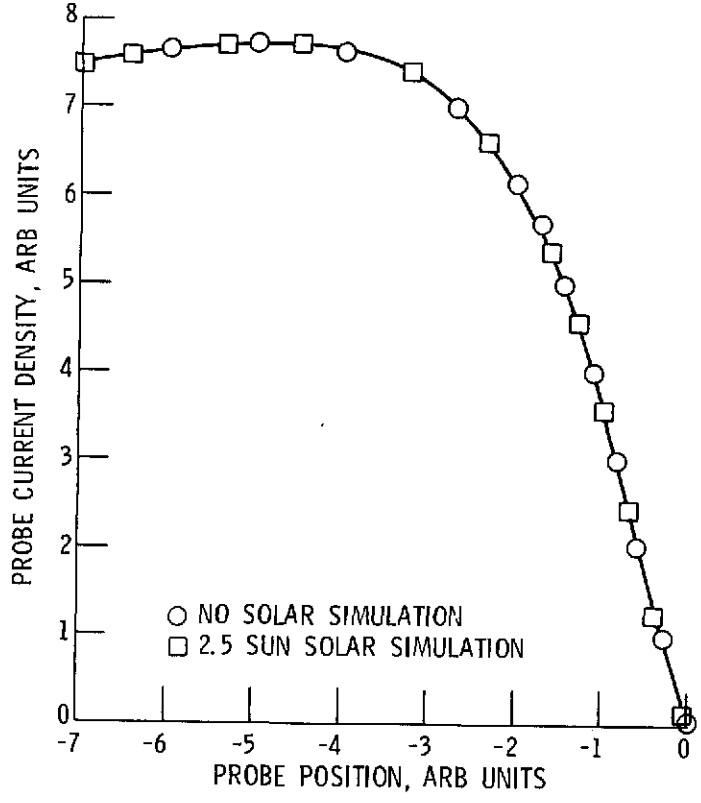


Figure 17. - Beam profile measured 100 cm from the thruster for $J_B$ = 1.9 A.

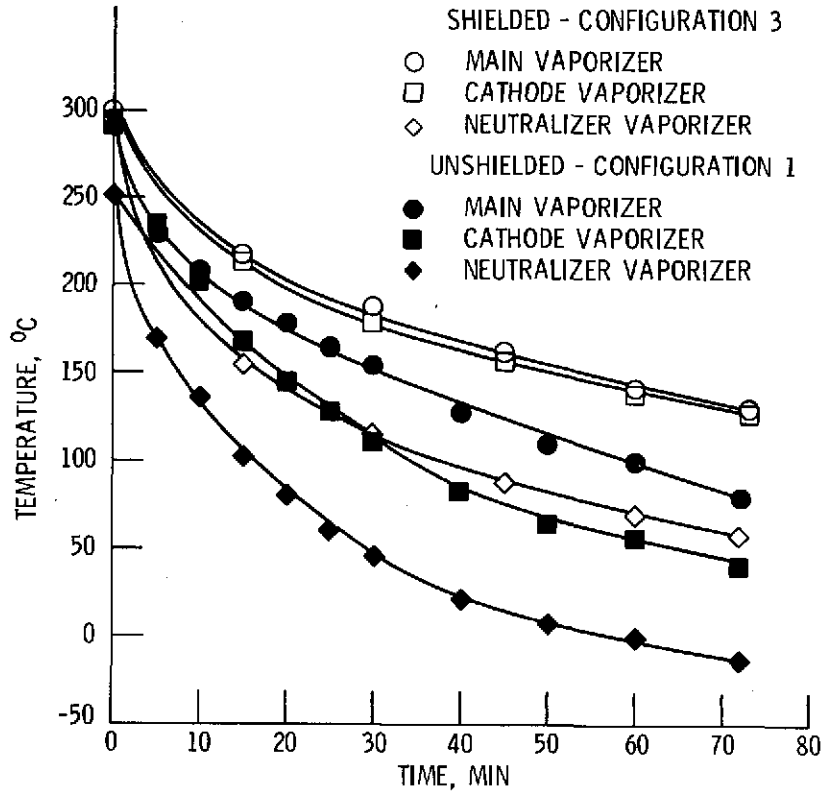


Figure 18. - Cooling curves during an eclipse simulation for thruster operating initially at full beam power.

NASA-Lewis